Electronic Supplementary Material (ESI) for Journal of Materials Chemistry A.
This journal is © The Royal Society of Chemistry 2018

Co_3O_4-doped Co/CoFe Nanoparticles Encapsulated in Carbon Shell as Bifunctional Electrocatalyst for Rechargeable Zn–Air Batteries

Tongtong Li,[a] Yongxin Lu,[a] Shuaishuai Zhao,[a] Zhi-Da Gao*[a] and Yan-Yan Song *[a]

[a]College of Sciences, Northeastern University, Shenyang 110004, China.

*Corresponding author: gaozd@mail.neu.edu.cn ; yysong@mail.neu.edu.cn

Thermodynamics of OER process in alkaline conditions: The surface (denoted as $*$) of the catalyst form the adsorbed OH and O species (denoted as OH* and O*, respectively) in the beginning:

$$OH^- + * \rightarrow OH^* + e^- \quad (1)$$

$$OH^* + OH^- \rightarrow O^* + H_2O + e^- \quad (2)$$

and then the O* react with OH^- forming the intermediate OOH*, which undergo reaction with additional OH^- producing H_2O and O_2:

$$O^* + OH^- \rightarrow OOH^* + e^- \quad (3)$$

$$OOH^* + OH^- \rightarrow O_2 + H_2O + e^- \quad (4)$$

the overall reaction can be expressed as

$$4OH^- \rightarrow O_2 + 2H_2O + 4e^- \quad (5)$$

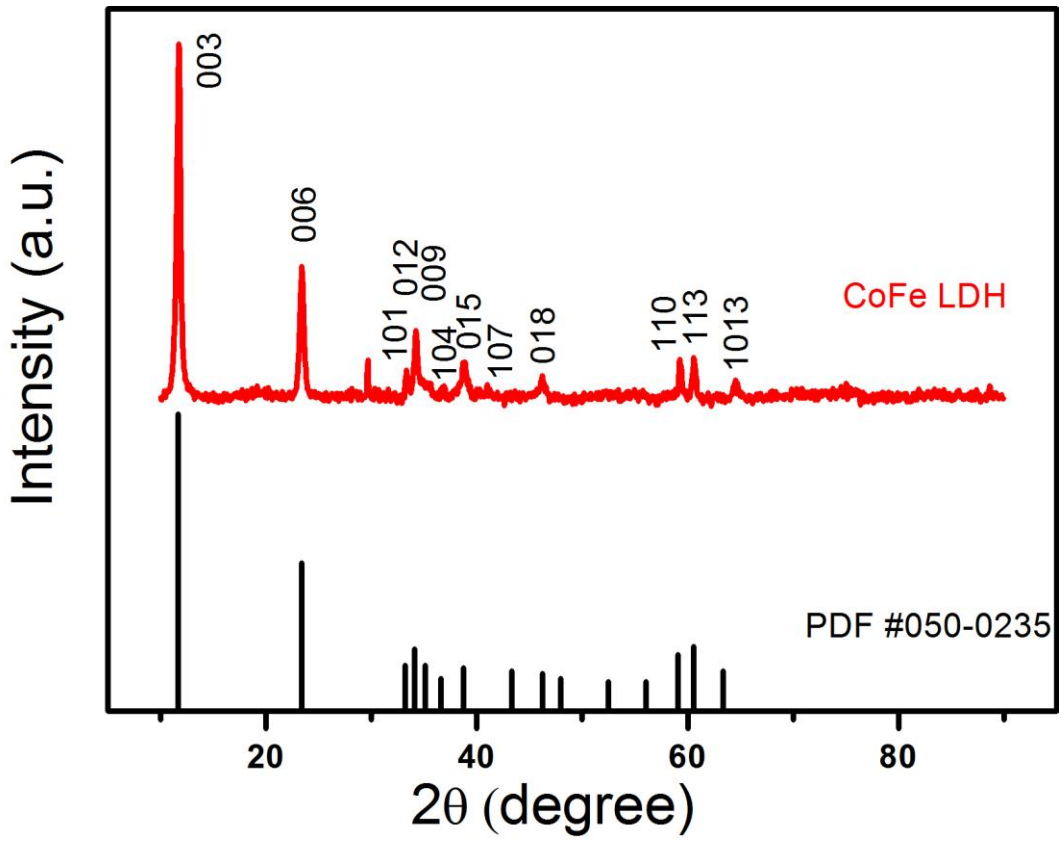

Figure S1. XRD patterns of the as-synthesized CoFe LDH.

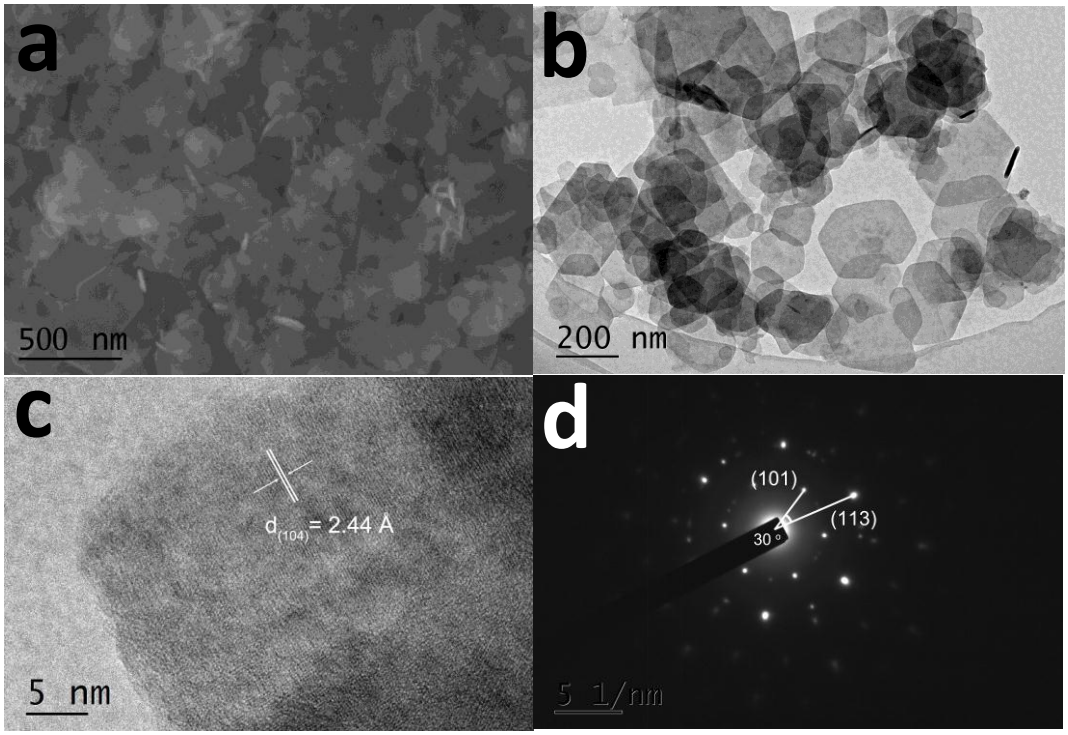

Figure S2. (a) SEM, (b) TEM, (c) HRTEM image, and (d) corresponding SAED patterns of CoFe LDH.

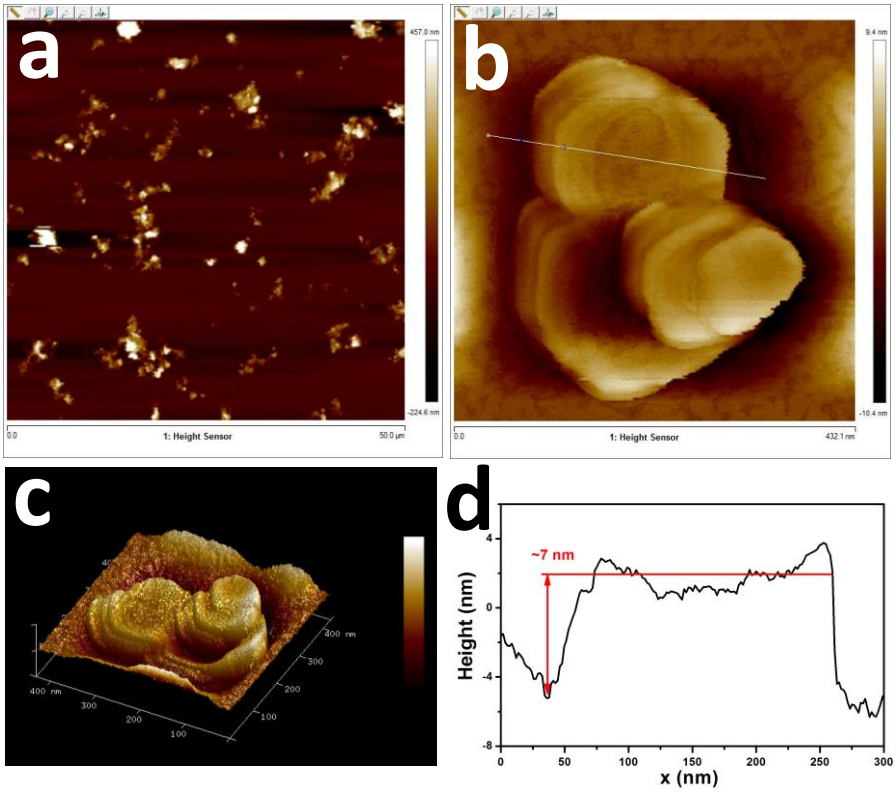

Figure S3. (a,b) AFM image (ScanAsyst mode) of several stacked LDH nanosheets on a Si wafers, (c) the corresponding 3D image of (b), and (d) the height mode profiles along the tracks shown in (b).

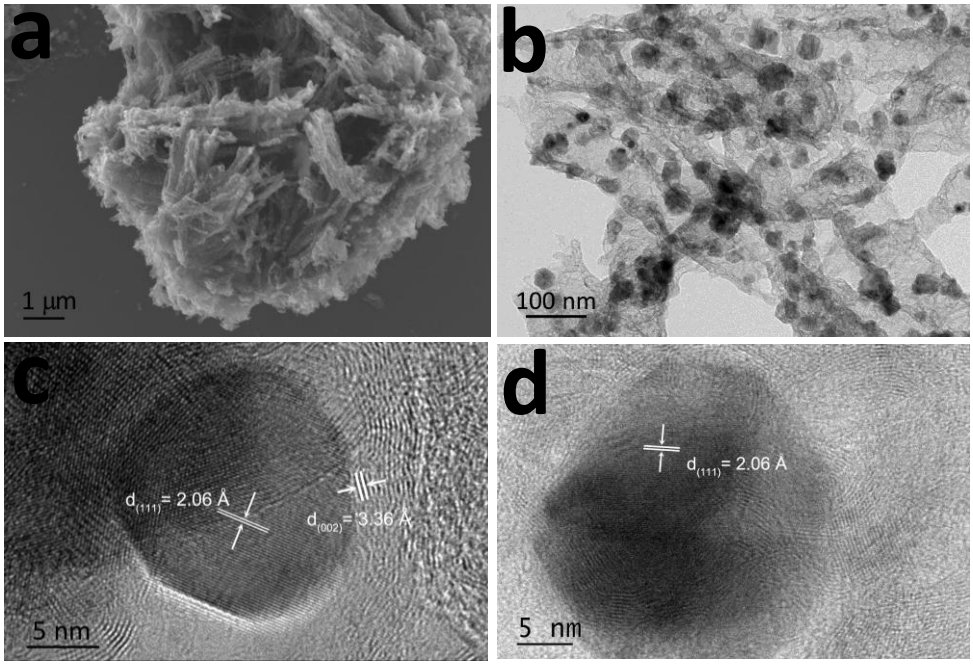

Figure S4. (a) SEM image, (b) TEM-image and (c,d) HR-TEM images of 3C-900.

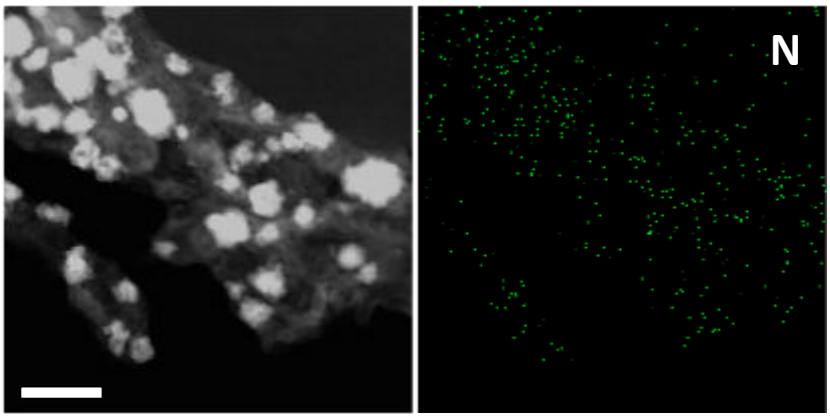

Figure S5. STEM-image and corresponding EDX mapping of N elements distributed in 3C-900. Scale bar, 100 nm.

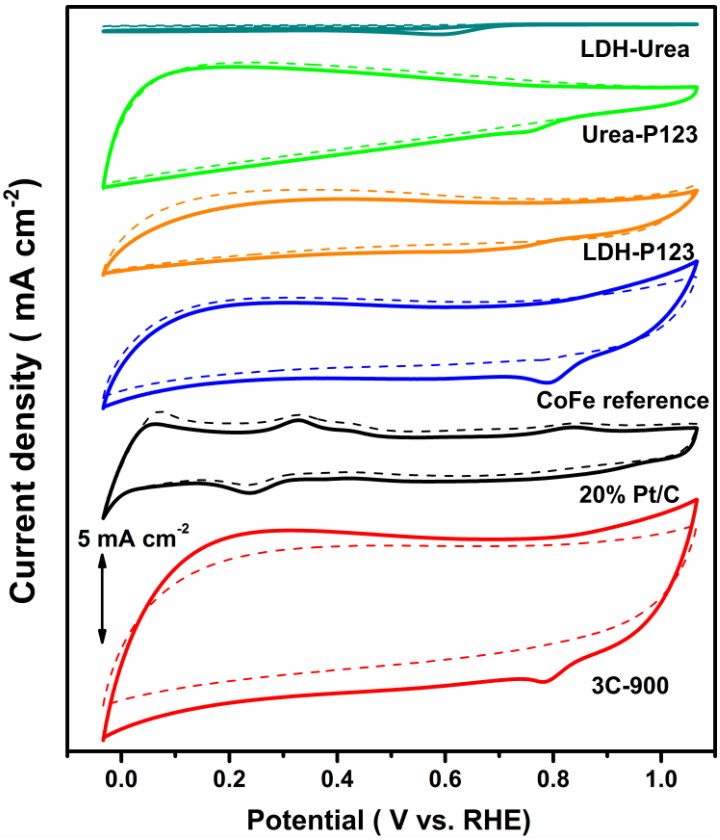

Figure S6. CVs of different catalysts in N_2- (dashed curves) and O_2-saturated (solid curves) 0.1 M KOH solution at a scan rate of 50 mV s^{-1}.

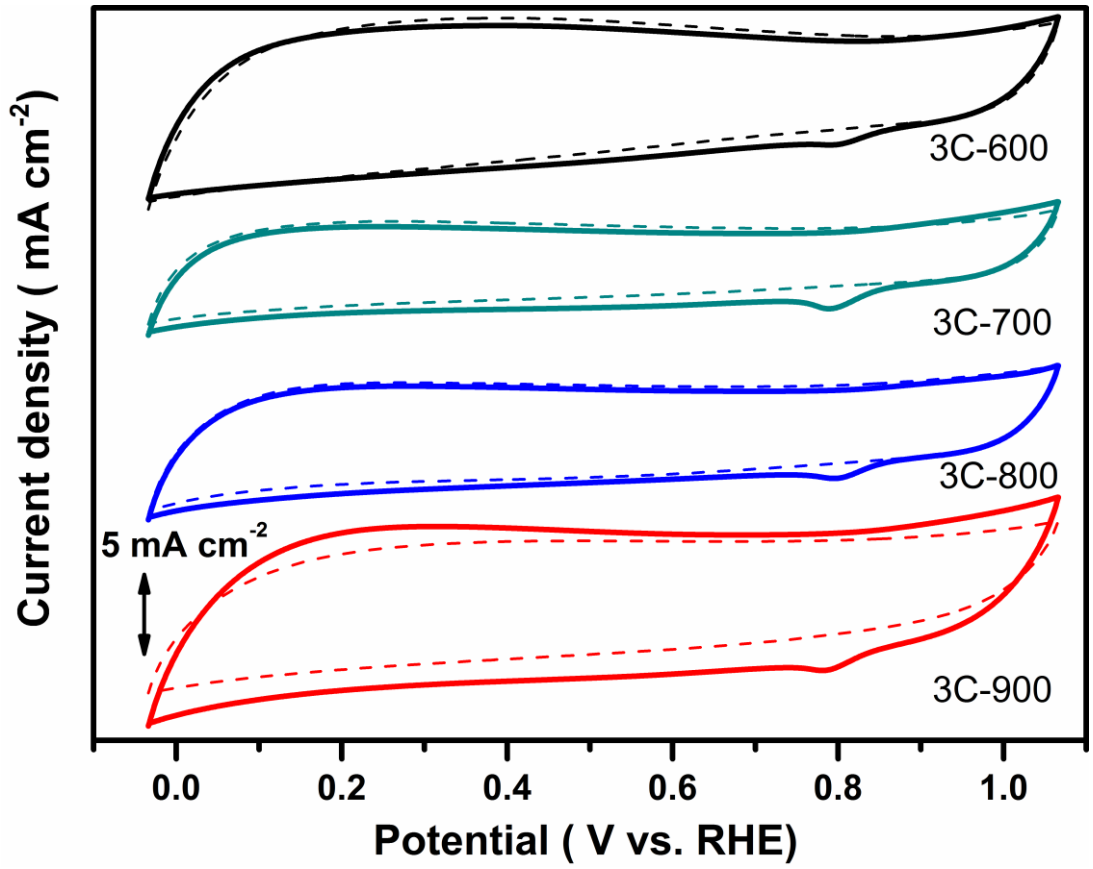

Figure S7. CVs of the catalysts prepared at different pyrolysis temperature in N_2- (dashed curves) and O_2-saturated (solid curves) 0.1 M KOH solution at a scan rate of 50 mV s^{-1}.

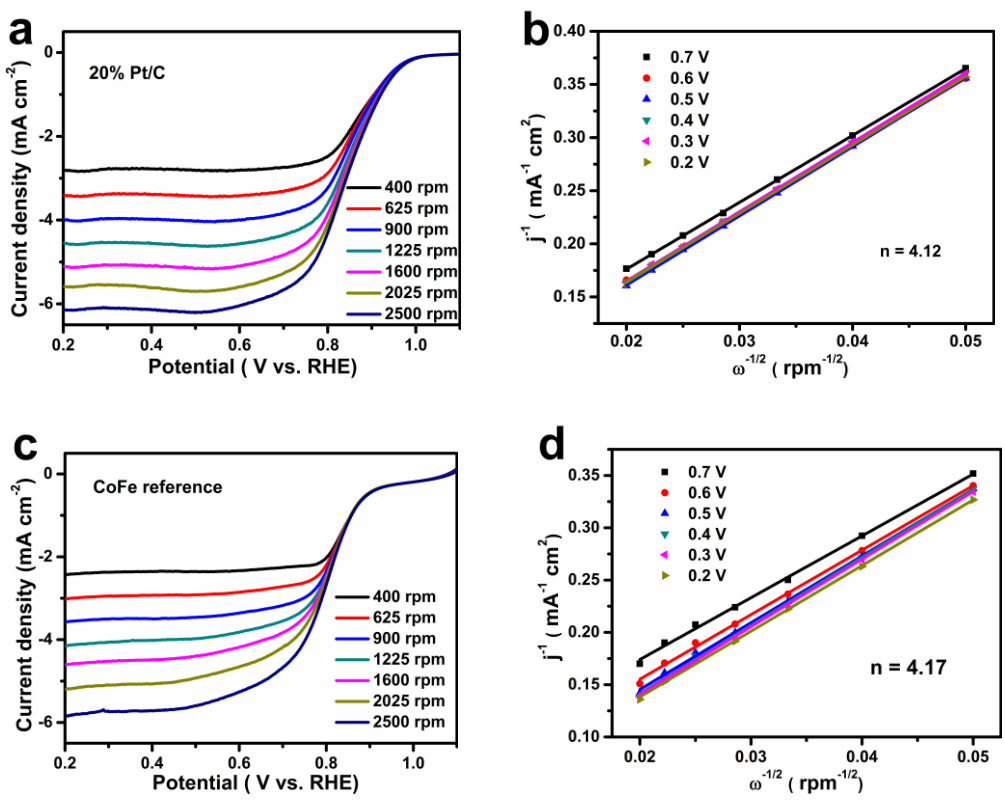

Figure S8. Polarization curves and corresponding K-L plots of (a, b) 20% Pt/C and (c, d) CoFe reference at various rotating speeds.

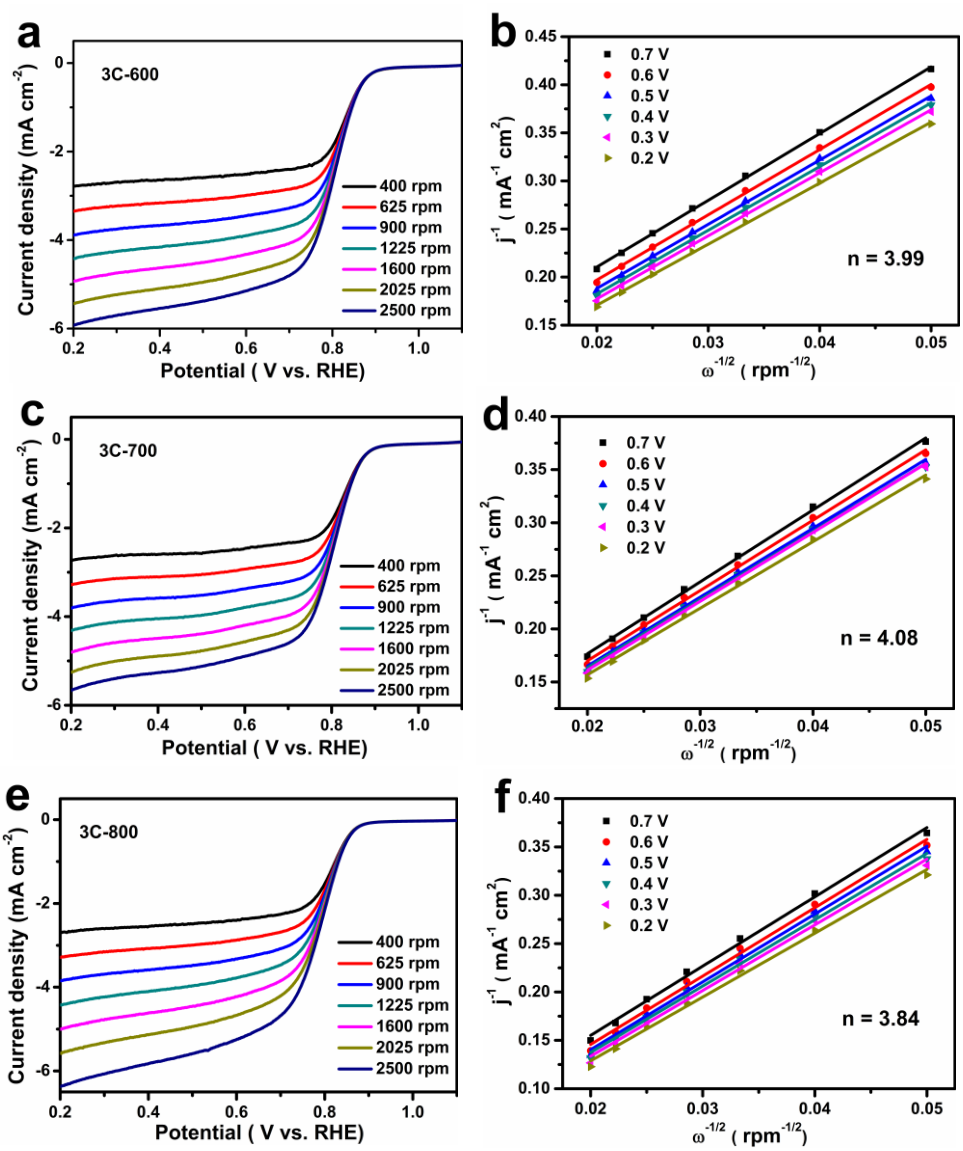

Figure S9. Polarization curves and corresponding K-L plots of (a, b) 3C-600, (c, d) 3C-700 and (e, f) 3C-800 at various rotating speeds.

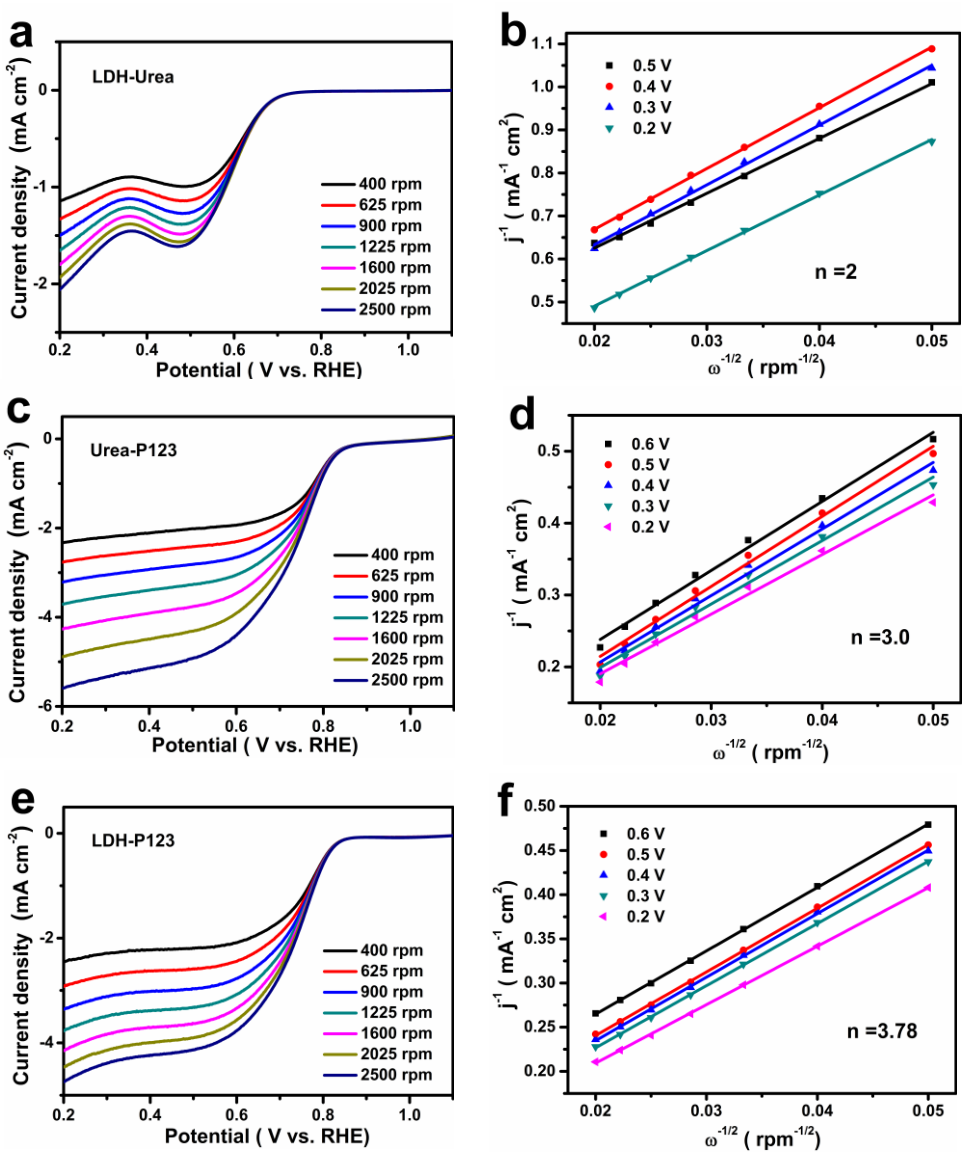

Figure S10. Polarization curves and corresponding K-L plots of (a, b) LDH-urea, (c, d) urea-P123 and (e, f) LDH-P123 at various rotating speeds.

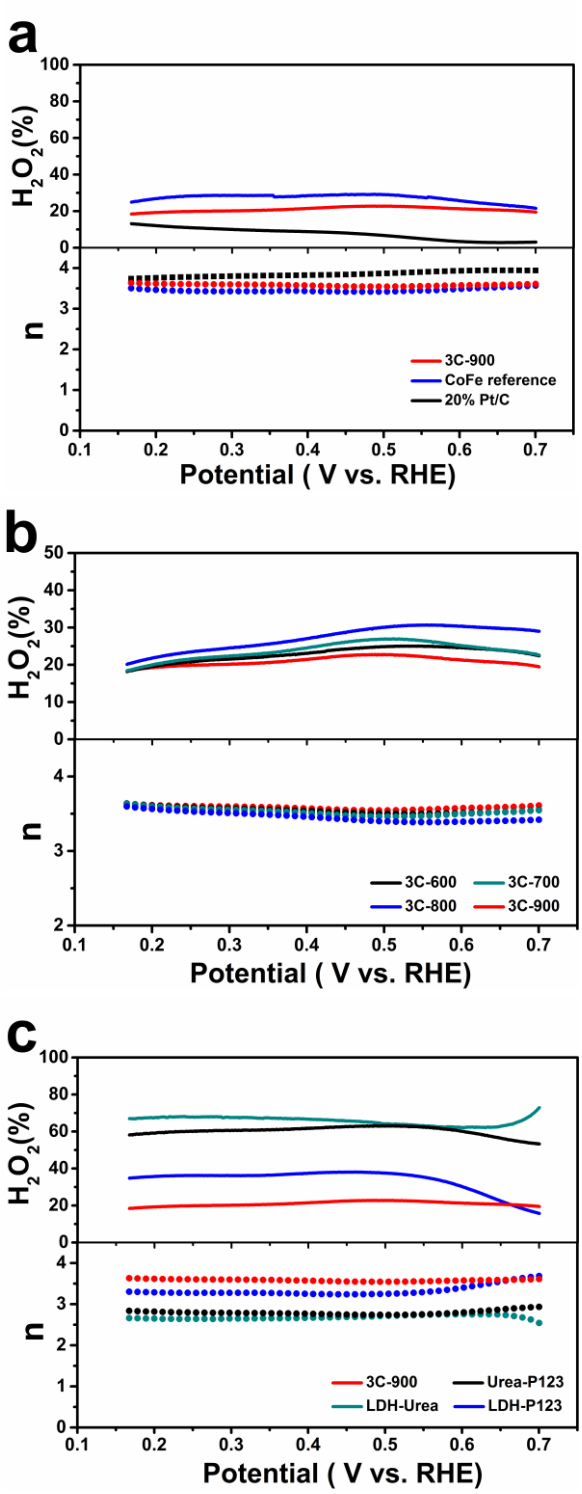

Figure S11. Peroxide yields and corresponding electron transfer number of various catalysts at different potentials based on RRDE data.

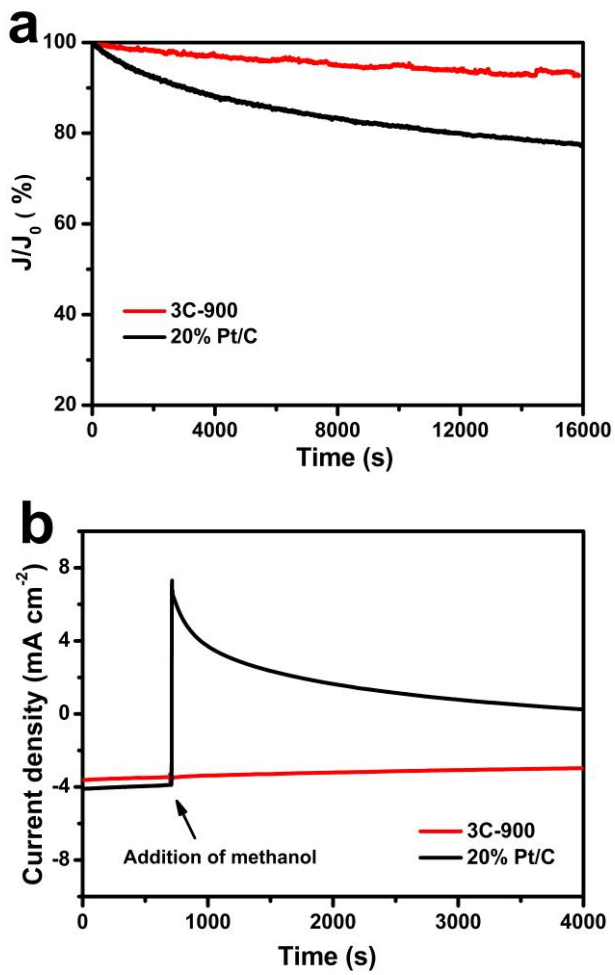

Figure S12. (a) Chronoamperometric responses of 3C-900 and 20% Pt/C at 0.75 V in O_2-saturated 0.1 M KOH. (b) Chronoamperometric responses of of 3C-900 and 20% Pt/C upon addition of 1 M methanol into O_2-saturated 0.1 M KOH at 0.75 V.

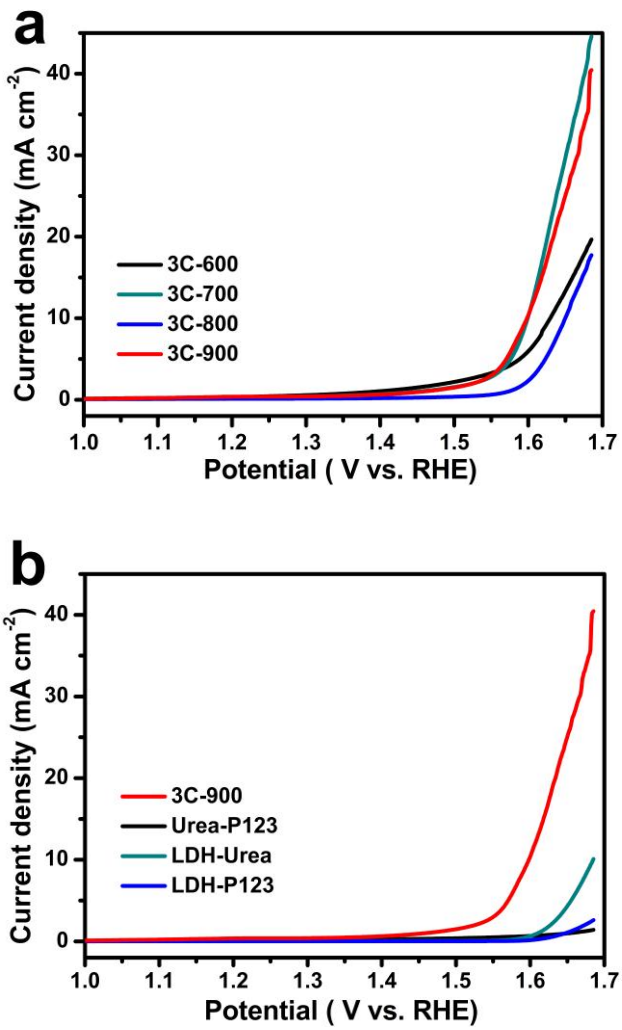

Figure S13. OER polarization curves of different catalysts in O_2-saturated 0.1 M KOH at 1600 rpm.

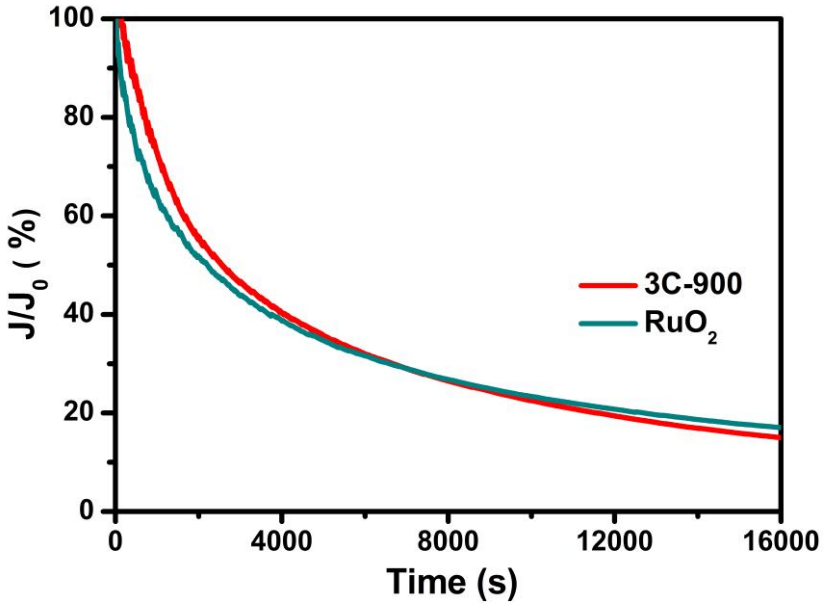

Figure S14. Chronoamperometric responses of 3C-900 and RuO_2 at 1.60 V in O_2-saturated 0.1 M KOH.

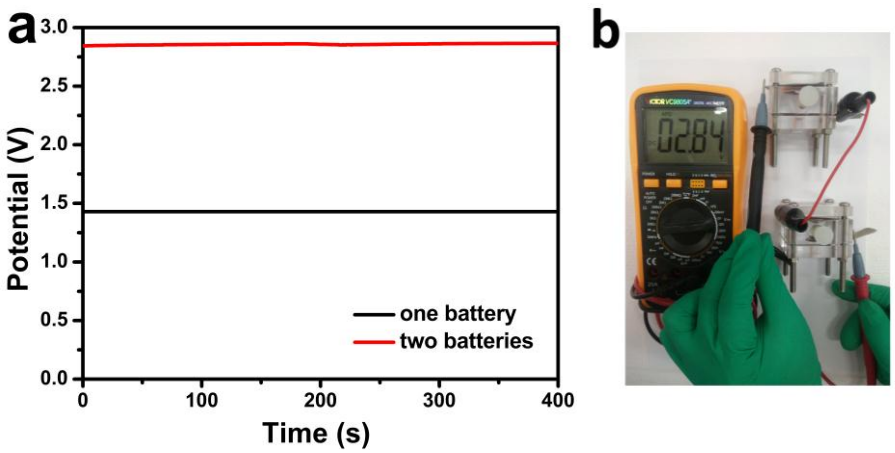

Figure S15. Open circuit potentials of a Zn-air battery and two batteries in series. (b) Photograph of two Zn-air batteries in series with an open circuit potential of 2.84 V.

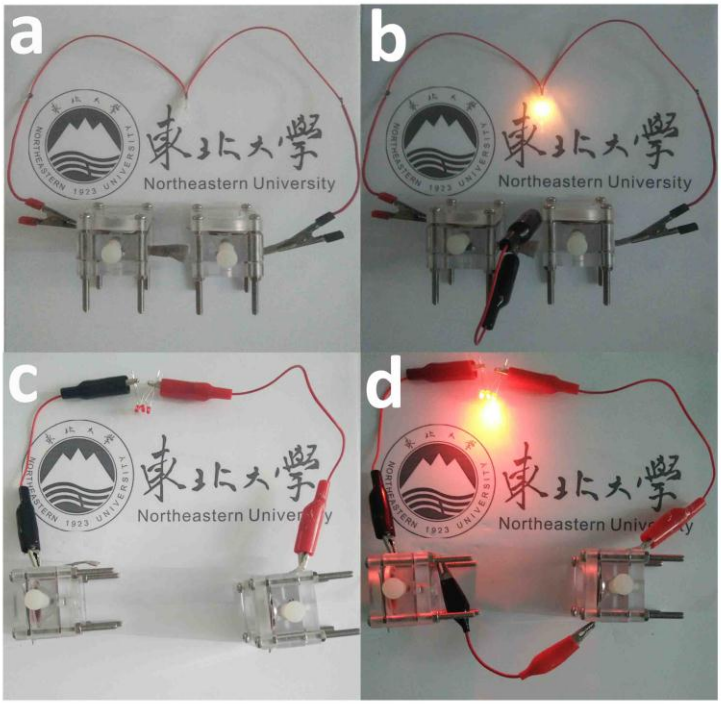

Figure S16. Optical images of a small bulb, and three red LED before (a,c) and after (b,d) being driven by two Zn–air batteries in series.

Table S1. The value of ΔE (ΔE = E_{j10} - E_{j-3}) for different catalysts.

Catalysts	E_{j-3} (V *vs*. RHE)	E_{j10} (V *vs*. RHE)	ΔE(V)	Ref.
3C-900	0.8153	1.5983	0.783	This work
CoFe	0.7943	1.6723	0.878	This work
RuO_2	0.3073	1.6113	1.304	This work
20% Pt/C	0.8303	>1.7653	>0.935	This work
CoS_2(400)/N,S-GO	0.79	1.61	0.82	1
Ni_3Fe/N-C sheets	0.78	1.62	0.84	2
Co@Co_3O_4/NC-1	0.80	1.65	0.85	3
Co/N-C-800	0.74	1.60	0.85	4
Co/NC	0.83	1.69	0.86	3
$Co_3FeS_{1.5}(OH)_6$	~0.721	1.588	~0.867	5
Mn_xO_y/N-C	0.81	1.68	0.87	6
Fe/Fe_2O_3@Fe-N-C-1000	0.79	1.66	0.87	7
Fe@N-C-700	0.83	1.71	0.88	8
N-Co_9S_8/G	0.76	1.64	0.88	9
S/N_Fe-27	0.87	1.78	0.91	10
Fe/N-CNTs	0.81	1.75	0.94	11

Reference

[1] P. Ganesan, M. Prabu, J. Sanetuntikul and S. Shanmugam, *ACS Catal.*, 2015, **5**, 3625-3637.

[2] G. Fu, Z. Cui, Y. Chen, Y. Li, Y. Tang and J. B. Goodenough, *Adv. Energy Mater.*, 2017, **7**, 1601172.

[3] A. Aijaz, J. Masa, C. Rösler, W. Xia, P. Weide, A. J. R. Botz, R. A. Fischer, W. Schuhmann and M. Muhler, *Angew. Chem., Int. Ed.*, 2016, **55**, 4087-4091.

[4] Y. Su, Y. Zhu, H. Jiang, J. Shen, X. Yang, W. Zou, J. Chen and C. Li, *Nanoscale*, 2014, **6**, 15080-15089.

[5] H.-F. Wang, C. Tang, B. Wang, B.-Q. Li and Q. Zhang, *Adv. Mater.*, 2017, **29**, 1702327.

[6] J. Masa, W. Xia, I. Sinev, A. Zhao, Z. Sun, S. Grützke, P. Weide, M. Muhler and W. Schuhmann, *Angew. Chem., Int. Edit.*, 2014, **53**, 8508-8512.

[7] Y. Zang, H. Zhang, X. Zhang, R. Liu, S. Liu, G. Wang, Y. Zhang and H. Zhao, *Nano Res.*, 2016, **9**, 2123-2137.

[8] J. Wang, H. Wu, D. Gao, S. Miao, G. Wang and X. Bao, *Nano Energy*, 2015, **13**, 387-396.

[9] S. Dou, L. Tao, J. Huo, S. Wang, L. Dai, *Energy Environ. Sci.*, 2016, **9**, 1320-1326.

[10] N. Ranjbar Sahraie, J. P. Paraknowitsch, C. Göbel, A. Thomas and P. Strasser, *J. Am. Chem. Soc.*, 2014, **136**, 14486-14497.

[11] Y. Liu, H. Jiang, Y. Zhu, X. Yang and C. Li, *J. Mater. Chem. A*, 2016, **4**, 1694-1701.